



# Microtubules and Dynein Regulate Human Neutrophil Nuclear Volume and Hypersegmentation During *H. pylori* Infection

Stephanie L. Silva-Del Toro<sup>1,2</sup> and Lee-Ann H. Allen<sup>1,2,3,4,5\*</sup>

<sup>1</sup> Inflammation Program of the University of Iowa, Iowa City, IA, United States, <sup>2</sup> Immunology Graduate Program of the University of Iowa, Iowa City, IA, United States, <sup>3</sup> Department of Internal Medicine, University of Iowa, Iowa City, IA, United States, <sup>4</sup> Department of Microbiology and Immunology, University of Iowa, Iowa City, IA, United States, <sup>5</sup> Iowa City VA Healthcare System, Iowa City, IA, United States

## OPEN ACCESS

### Edited by:

Liwu Li,  
Virginia Tech, United States

### Reviewed by:

Marco A. Cassatella,  
University of Verona, Italy  
Tobias Dallenga,  
Research Center Borstel  
(LG), Germany

### \*Correspondence:

Lee-Ann H. Allen  
lee-ann.allen@health.missouri.edu  
orcid.org/0000-0001-8929-6968

### Specialty section:

This article was submitted to  
Molecular Innate Immunity,  
a section of the journal  
Frontiers in Immunology

**Received:** 13 January 2021

**Accepted:** 24 February 2021

**Published:** 22 March 2021

### Citation:

Silva-Del Toro SL and Allen L-AH  
(2021) Microtubules and Dynein  
Regulate Human Neutrophil Nuclear  
Volume and Hypersegmentation  
During *H. pylori* Infection.  
*Front. Immunol.* 12:653100.  
doi: 10.3389/fimmu.2021.653100

Neutrophils (also called polymorphonuclear leukocytes, PMNs) are heterogeneous and can exhibit considerable phenotypic and functional plasticity. In keeping with this, we discovered previously that *Helicobacter pylori* infection induces N1-like subtype differentiation of human PMNs that is notable for profound nuclear hypersegmentation. Herein, we utilized biochemical approaches and confocal and super-resolution microscopy to gain insight into the underlying molecular mechanisms. Sensitivity to inhibition by nocodazole and taxol indicated that microtubule dynamics were required to induce and sustain hypersegmentation, and super-resolution Stimulated Emission Depletion (STED) imaging demonstrated that microtubules were significantly more abundant and longer in hypersegmented cells. Dynein activity was also required, and enrichment of this motor protein at the nuclear periphery was enhanced following *H. pylori* infection. In contrast, centrosome splitting did not occur, and lamin B receptor abundance and ER morphology were unchanged. Finally, analysis of STED image stacks using Imaris software revealed that nuclear volume increased markedly prior to the onset of hypersegmentation and that nuclear size was differentially modulated by nocodazole and taxol in the presence and absence of infection. Taken together, our data define a new mechanism of hypersegmentation that is mediated by microtubules and dynein and as such advance understanding of processes that regulate nuclear morphology.

**Keywords:** neutrophils, plasticity, hypersegmentation, microtubules, dynein, lamin B receptor

## INTRODUCTION

Neutrophils or polymorphonuclear leukocytes (PMNs) are the most abundant white blood cell in circulation, are the first leukocytes to be recruited to sites of infection, and are essential for innate host defense (1–3). PMNs are also short-lived and terminally differentiated and are notable for their peculiar, segmented nuclei comprised of three or four interconnected lobes (2, 4). Until recently, PMNs were thought to be a homogeneous population of cells with a singular phenotype. However, this notion has been fundamentally changed by the discovery of PMN plasticity and the characterization of different cell populations that differ in maturation state, density, functional properties and nuclear morphology (5–8). From tumor-associated neutrophils to professional

antigen presenting cells involved in adaptive immunity, to bacterial and parasitic infections and sepsis as well as autoimmune disease, a spectrum of pro-inflammatory, regulatory and suppressive PMNs have been described. Hypersegmented PMN subsets were first noted in the murine tumor microenvironment and more recently have been identified in patients with lung and ovarian cancer, obstructive lung disease, juvenile inflammatory arthritis, hyperthermia, and during experimental endotoxemia (9–15). Previously thought to occur only in response to *in vivo* cues, we discovered that infection of human neutrophils with the ulcer and gastric cancer-causing Gram-negative bacterium *Helicobacter pylori* can induce N1-like subtype differentiation of human neutrophils *in vitro* that is notable for profound nuclear hypersegmentation, proinflammatory cytokine secretion, a CD62L<sup>dim</sup>, CD16<sup>bright</sup>, CD11b<sup>bright</sup>, CD66b<sup>bright</sup>, CD63<sup>bright</sup> surface phenotype and a 72 h lifespan (16). More recently, Ohms et al. (17) also attempted *in vitro* polarization of human neutrophils, but their analysis did not include examination of nuclear morphology.

Hypersegmentation is defined as 5% of PMNs with five nuclear lobes or any single cell with six lobes or more and was described first in the context of folate or vitamin B12 deficiency which impairs DNA synthesis during neutrophil development in the bone marrow (18–20). Conversely, the mechanisms that mediate hypersegmentation of PMN subsets are unknown. During *H. pylori* infection, hypersegmentation is not linked to folate or vitamin B12, but does require direct infection and both host and bacterial transcription and protein synthesis (16). Herein, we used this tractable system to gain fundamental new insight into the mechanisms that control neutrophil nuclear morphology.

## MATERIALS AND METHODS

### Cultivation of *H. pylori*

*H. pylori* strain NCTC11637 (ATCC 43504) was grown for 24 h under humidified, microaerophilic conditions (5% O<sub>2</sub>, 10% CO<sub>2</sub>, 85% N<sub>2</sub>) at 37°C on trypticase soy agar (Difco, Franklin Lakes, NJ) containing 5% defibrinated sheep blood (Remel, Lenexa, KS) and supplemented with 5 mg/L cefsulodin, 5 mg/L trimethoprim, and 10 mg/L vancomycin (21). Bacteria were harvested from plates, washed twice in PBS containing 1 mM glucose and quantified by measuring absorbance at 600 nm.

### Ethics Statement

Heparinized venous blood was obtained from healthy adult donors who provided written informed consent using procedures approved by the Institutional Review Board of the University of Iowa (IRB #200307026).

### PMN Isolation and Bacterial Infection

PMNs were isolated by dextran sedimentation and Ficoll-Hypaque gradient separation followed by hypotonic lysis of erythrocytes (22). Neutrophils were routinely 95–98% pure with eosinophils as the major contaminant. Cells were resuspended at  $2 \times 10^6$  cells/mL in HEPES-buffered RPMI-1640 medium (Lonza, Walkersville, MD) supplemented with 10% heat-inactivated

FBS (HyClone Laboratories, Pittsburgh, PA) and 2 mM L-glutamine (Lonza, Walkersville, MD) and then incubated in suspension at 37°C under microaerophilic conditions in the presence or absence of *H. pylori* at a multiplicity of 5 bacteria/cell. Replicate experiments utilized PMNs from different donors.

### Inhibitor Treatment

Drugs at the following final concentrations were added at time zero unless otherwise indicated: nocodazole (Calbiochem, San Diego, CA) at 10 μM, taxol (Sigma, Burlington, MA) at 1 μM, and ciliobrevin D (EMD Millipore Sigma, Burlington, MA) at 20 μM.

### Hema-3 Staining and Nuclear Morphology Analysis

PMNs were attached to coverslips by cytocentrifugation and immediately stained using Hema-3 Stat Pack reagents (Thermo Fisher Scientific, Waltham, MA) (16, 23). Nuclear morphology was analyzed by light microscopy (Zeiss Axioplan 2 with Axiovision software, Carl Zeiss Inc., Thornwood, NY) as we described (16).

### Immunofluorescence and Confocal Microscopy

Cells were attached to acid washed coverslips coated with human serum as we described (24, 25) and then gently washed with PBS prior to fixation, with conditions optimized for detection of different antigens. Our standard conditions were used to detect lamin B receptor (LBR) and lamin B1 (25). In brief, cells were fixed in 10% formalin for 15 min, permeabilized with cold methanol-acetone (1:1) for 5 min, rinsed with PBS containing 0.5 mg/mL NaN<sub>3</sub> and 5 mg/mL BSA (PAB) and then blocked overnight in PAB containing 10% horse serum. To detect dynein and microtubules (MTs), cells were fixed and permeabilized as described by Ding et al. (26), with minor modifications. Specifically, cells were fixed in 4% paraformaldehyde (PFA) immediately followed by addition of 0.2% glutaraldehyde, for a final concentration of 2 and 0.1%, respectively, in PBS containing 0.002% NaN<sub>3</sub> (PBSa) and incubated for 15 min at room temperature. After a PBSa wash, cells were permeabilized in 0.5% SDS in PBSa, and then blocked as described above. To visualize the ER, cells were fixed with 4% PFA for 15 min and then permeabilized with 0.02% Triton X-100 for 5 min, both at room temperature.

Blocked cells were stained with a 1/1,000 dilution of affinity-purified goat anti-*H. pylori* polyclonal antibodies (pAb) (SeraCare, Milford, MA), 1/200 mouse anti-γ-tubulin mAb (clone GTU-88, Abcam, Cambridge, MA), 1/500 rabbit anti-α-tubulin (EP1332Y, Abcam, Cambridge, MA), 1/100 mouse anti-dynein (74.1, Abcam, Cambridge, MA), 1/100 mouse anti-protein disulfide-isomerase (PDI) (RL77, Thermo Fisher Scientific, Waltham, MA), 1/1,000 rabbit anti-Lamin B Receptor (E398L, Abcam, Cambridge, MA), or 1/1,000 pAb rabbit anti-lamin B1 (Abcam, Cambridge, MA) as we described (25). Affinity-purified F(ab')<sub>2</sub> secondary

antibodies were obtained from Jackson ImmunoResearch Laboratories (West Grove, PA) and used at 1/200 dilution. In each case, specificity of staining was determined by omission of primary antibodies. Background signals obtained from secondary antibodies alone are shown in **Supplementary Figure 1**.

Coverslips were mounted to slides using Prolong Diamond Antifade mountant with DAPI (Invitrogen, Carlsbad, CA) and analyzed using a Zeiss LSM880 confocal microscope, with a 1 AU pinhole aperture and utilizing the Zeiss Zen acquisition software. Z-stacks were obtained of each cell and 3D reconstructions and processing used Oxford Bitplane Imaris Software (version 9.2.1). At least 100 cells per condition were analyzed for each condition and donor.

### Stimulated Emission Depletion Microscopy (STED)

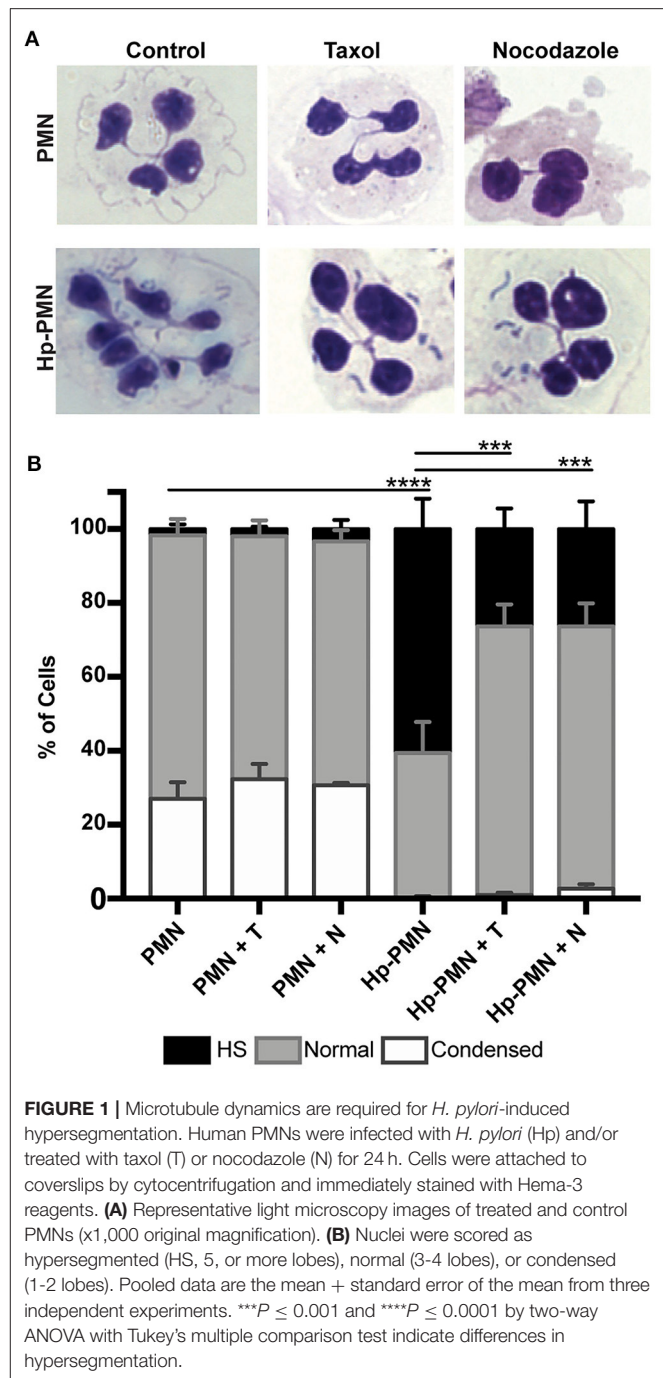
PMNs were attached to serum-coated, acid washed #1.5 German glass coverslips (Electron Microscopy Sciences, Hatfield, PA), fixed and permeabilized as described above and stained with 1/100 goat anti-rabbit LBR (clone E398L, Abcam, Cambridge, MA) or 1/25 purified rat anti-tyrosinated  $\alpha$ -tubulin (clone YL1/2, Millipore Sigma, Burlington, MA) as above, except incubation with primary antibodies was increased to 2 h. Z-stack images were acquired using a Leica SP8 STED Super Resolution Microscope and LAS X software (Leica Microsystems, Buffalo Grove, IL). A resolution of 40–50 nm was obtained after processing using Huygens Professional Software deconvolution wizard (version 19.04) set to a maximum of 40 iterations. Volume, area and microtubule quantifications were done using Oxford Bitplane Imaris Software (version 9.2.1) surface and filament extensions.

### Flow Cytometry

After incubation in Intracellular Fixation Buffer (Thermo Fischer Scientific, Waltham, MA) for 30 min at room temperature and permeabilization with cold 100% methanol on ice for 30 min, cells were stained with FITC-conjugated anti-LBR mAb (clone e398L, Abcam, Cambridge, MA) diluted 1/50 in blocking buffer (1% FBS in PBS). After washing, cells were resuspended in PBS and 10,000 events/sample were acquired using an Accuri C6 Cytometer (BD Biosciences, East Rutherford, NJ) followed by FlowJo V10 analysis.

### Western Blotting

Whole cell lysates were prepared as we described (27). Proteins were separated on NuPAGE™ 4–12% Bis-Tris protein gels (Invitrogen, Carlsbad, CA) and then transferred to polyvinylidene fluoride membranes using a Trans-Blot Turbo (Bio-Rad, Hercules, CA). Blocked membranes were probed with 1/1,000 anti- $\alpha$ -tubulin (EP1332Y, Abcam, Cambridge, MA) or 1/1,000 anti-dynein (74.1, Abcam, Cambridge, MA) and then stripped and re-probed with 1/2,000 anti-GAPDH (6C5, Calbiochem, San Diego, CA). HRP-conjugated secondary antibodies were from GE Healthcare (Chicago, IL) and Bio-Rad (Hercules, CA) and



were used at 1/2,000. Bands were detected using West Femto reagents (Thermo Fischer Scientific, Waltham, MA) with Li-Cor Odyssey imaging and Image Studio Software analysis.

### Statistical Analysis

All experiments were performed at least three times. Analyses utilized GraphPad Prism 7 or 8 with  $P < 0.05$  considered statistically significant. See figure legends for details.

## RESULTS

### Microtubule Dynamics Are Required to Induce Hypersegmentation

To test the hypothesis that MTs are required for *H. pylori*-induced nuclear hypersegmentation PMNs were treated with taxol or nocodazole at time zero in the presence and absence of bacteria and nuclear morphology was assessed at 24 h using Hema-3 staining and light microscopy. As expected, the majority of uninfected PMNs had normal lobed nuclei and a subset of cells had condensed spherical nuclei indicative

of progression to apoptosis (16, 23). In marked contrast, the majority of infected cells (Hp-PMNs) contained as many as 19 nuclear lobes and are defined as hypersegmented (16). However, when MTs were bundled by taxol or depolymerized by nocodazole (confirmed in **Supplementary Figure 2A**) hypersegmentation was significantly inhibited (**Figures 1A,B**). Based on these data, we conclude that MT dynamics were required for *H. pylori*-induced hypersegmentation but not for sustained lobulation of mature neutrophil nuclei or for the nuclear condensation that accompanies progression to apoptosis.

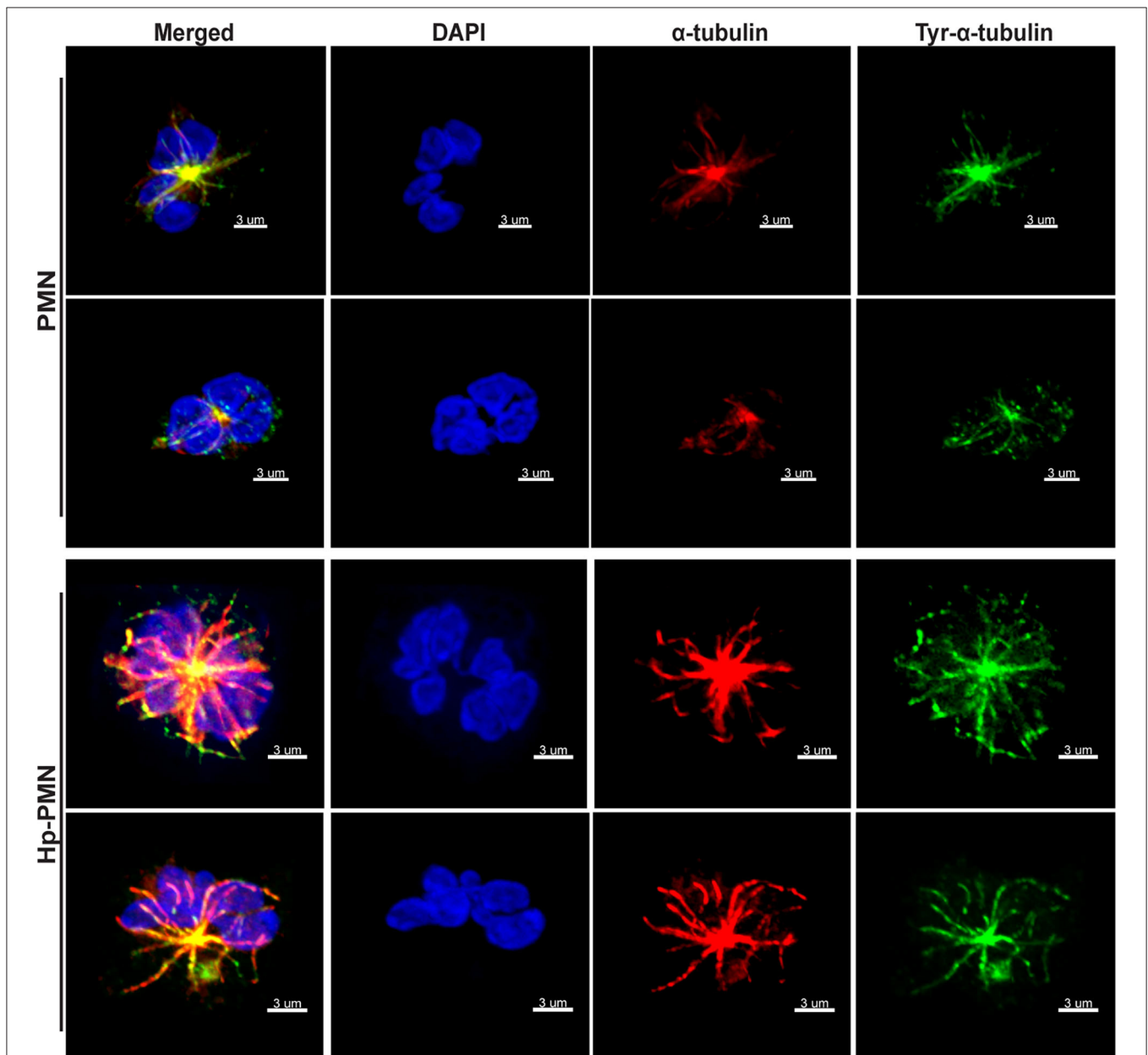


**FIGURE 2** | MTs appear to be more abundant in infected PMNs and tyrosination is prevalent throughout MTs independent of infection. Control and infected PMNs were analyzed by confocal microscopy at 24 h after triple-staining to detect DNA (DAPI, blue),  $\alpha$ -tubulin (Alexa Fluor 549, red), and tyrosinated  $\alpha$ -tubulin (FITC, green). Images are representative 3D reconstructions of confocal Z-stacks from three independent experiments. Scale bar = 3  $\mu$ m (x1,000 original magnification).

## Microtubules Are More Abundant Following *H. pylori* Infection and Microtubule Dynamics Are Required for Sustained Hypersegmentation

Next, we used immunofluorescence and confocal microscopy to detect MTs in control and infected PMNs after 24 h at 37°C. Staining with anti- $\alpha$ -tubulin antibodies showed that MTs radiate from the perinuclear microtubule organizing center (MTOC) in both control and infected cells, and similar results were obtained using antibodies specific for tyrosinated  $\alpha$ -tubulin, a marker of dynamic MTs (28) (Figure 2). Staining for the MTOC marker  $\gamma$ -tubulin (29) demonstrated that each cell contained a single focus for MT polymerization (Supplementary Figure 2B), excluding centrosome splitting as a mechanism contributing to hypersegmentation in our system (30).

As our confocal data suggested that MTs may be more abundant in Hp-PMNs (Figure 2), we analyzed these structures in detail using super-resolution STED microscopy. Representative images are shown in Figure 3A, along with quantitation of MT number (Figure 3B) and length (Figures 3C,D) determined using Imaris software (Figure 3E, schematic). These data demonstrate that MTs were more abundant and longer in Hp-PMNs, results that are also apparent by comparison of Supplementary Videos 1, 2. Nevertheless, the overall abundance of  $\alpha$ -tubulin in control and infected cells was unchanged as judged by western blotting (data not shown).

To determine if hypersegmentation was reversible, we added taxol or nocodazole to PMNs at 18 h post-infection (hpi), and then processed cells for microscopy 6 h later (at 24 hpi). As shown in Figure 4, ~70% of Hp-PMN were hypersegmented by 18 hpi, but only a small fraction of cells retained this morphology after drug treatment, and as such were indistinguishable from the uninfected controls (Figures 4A,B).

To gain further insight into the kinetics of MT rearrangements, uninfected and infected cells that had previously been treated with taxol were analyzed by microscopy 5–60 min after drug washout. In uninfected PMNs, MTs remained bundled 15 min after taxol was removed and had only partially rearranged after 30–60 min (Figure 4C). Conversely, MTs rearranged very rapidly in Hp-PMN, as bundled MTs were diminished or absent by 5 min and normal MT asters radiating from the MTOC were restored by 15 min (Figure 4D). These data demonstrate that hypersegmentation was reversible, and that MT dynamics were required to sustain as well as induce this atypical nuclear morphology.

## Dynein Localization and Activity in Hypersegmentation

Cytoplasmic dynein is a motor protein that mediates retrograde transport along MTs and contributes to centrosome and nuclear positioning (31). We show here that a significant reduction in nuclear hypersegmentation was observed in Hp-PMNs treated with the dynein AAA<sup>+</sup> ATPase inhibitor ciliobrevin D (32), whereas nuclear morphology of the uninfected control PMNs

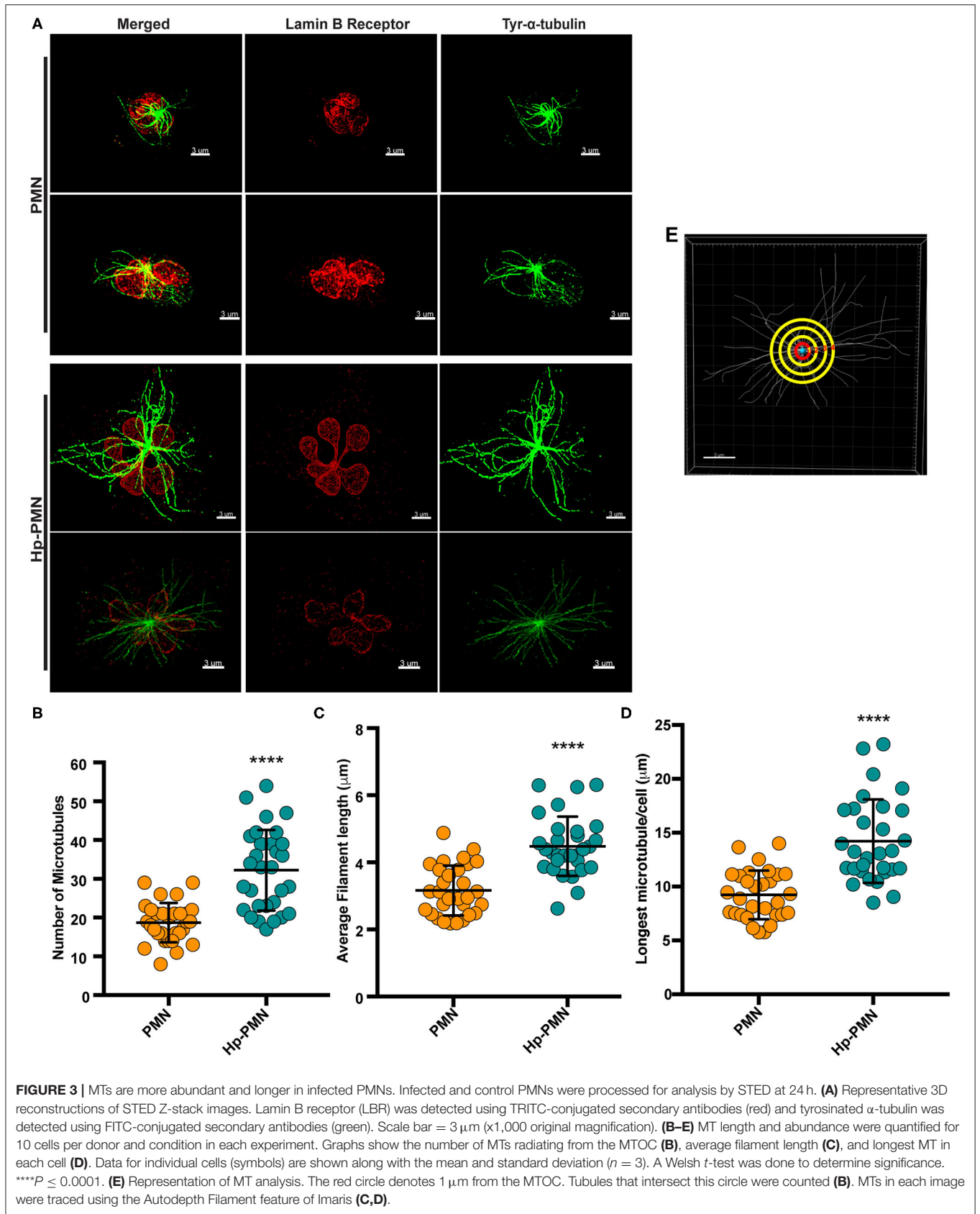
was unchanged (Figures 5A,B). Confocal microscopy revealed that although dynein was diffusely distributed throughout control PMNs, in agreement with published data (33), it appeared more abundant on nuclei of Hp-PMNs (Figure 5C). Nonetheless, total dynein levels did not change with infection or across time (Figure 5D). Thus, dynein activity and potentially protein relocalization contributed to hypersegmentation in our system.

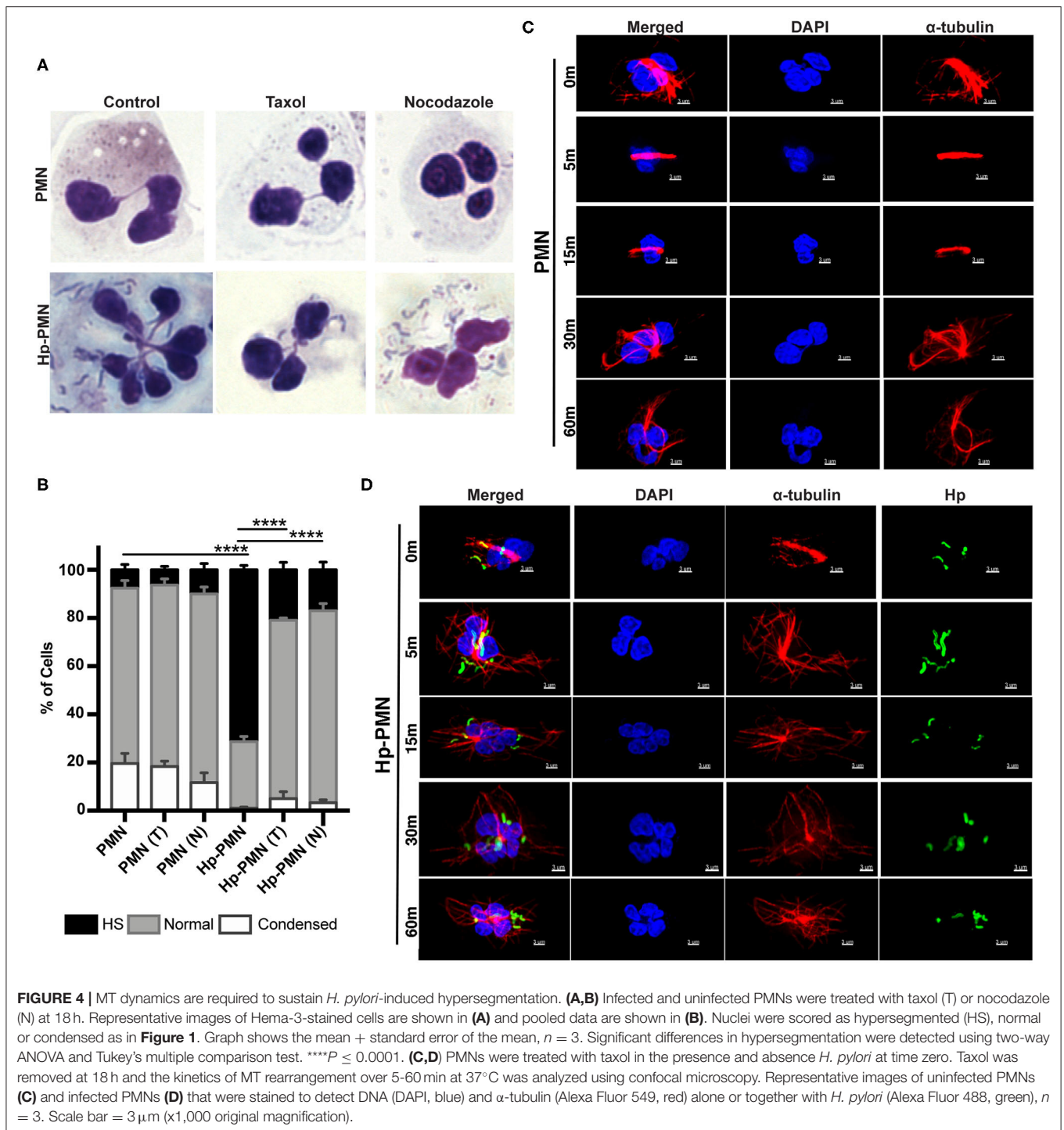
## Lamin B Receptor and Lamin B1 Are Distributed Throughout the Nuclear Envelope

LBR is an abundant multi-spanning integral protein of the inner nuclear membrane that binds directly to intermediate filament proteins of the lamin B family and also interacts with heterochromatin, thereby anchoring the lamina and DNA to the membrane (18, 34). Confocal imaging demonstrated that both LBR and lamin B1 were distributed throughout the nuclear envelopes of control as well as Hp-PMNs (Figures 6A,B) and similar results were obtained for lamin B2 (data not shown). It is established that LBR levels increase during neutrophil development and that *LBR* gene dosage directly influences the abundance of this protein and PMN nuclear morphology (34). Specifically, neutrophils from people with Pelger-Huet anomaly have only one functional copy of *LBR* and are hyposegmented (bi-lobed), whereas human PMNs with three functional *LBR* alleles are hypersegmented (34). With this in mind, we quantified LBR using flow cytometry (Figure 6C) and found that control and infected cells were indistinguishable at 8 h. At 24 h, LBR was slightly elevated in Hp-PMN and slightly reduced in control PMNs, likely because some of the latter cells were apoptotic (16) (Figures 1B, 4B, 5B), but these changes were not significant relative to the 8 h baseline. As LBR traffics to the nuclear membrane from the ER (18), we also examined this organelle using antibodies to the marker protein PDI but detected no discernable differences between Hp-PMN and the uninfected controls (Supplementary Figure 3).

## Microtubule-Dependent Nuclear Enlargement Precedes Hypersegmentation

Next, we stained cells to detect LBR and utilized STED super-resolution microscopy to obtain detailed analyses of nuclear size and shape at 8 and 24 h. Volume and surface area were measured on Z-stack reconstructions after surface rendering, depicted in Figures 6D,E and Supplementary Videos 3–6. Uninfected PMN nuclei were very similar to one another in morphology (Figures 7A,D), volume (Figures 7B,E), and surface area (Figures 7C,F) at both time points and for all donors tested. However, it is important to note that only segmented control cells were included in this analysis and cells with condensed apoptotic nuclei were excluded. In marked contrast, the morphology of infected PMN nuclei was very heterogeneous, in agreement with the data shown in Figures 1A, 4A, 5A, 6A,B and our previous work (16). Moreover, significant increases in nuclear volume and surface area were observed in Hp-PMNs as early as 8 hpi (Figures 7B,C) and were sustained to at least 24 hpi (Figures 7E,F). As we have shown that only a small fraction of





cells (~15%) are hypersegmented at 8 hpi (16), these new data demonstrate that changes in nuclear volume and surface area preceded hypersegmentation and were sustained thereafter, and as such are defining characteristics of Hp-PMNs.

Finally, we examined the effects of MTs on nuclear volume at 24 h, performing similar analyses of control and infected cells treated with nocodazole or taxol at time zero (**Figures 7G,H**)

and with comparison to the no-drug controls (**Figures 7E,G,H**). The data indicate that bacteria-driven nuclear enlargement was nearly ablated by nocodazole (**Figures 7G,H**). On the other hand, taxol treatment increased nuclear volume to a similar extent as *H. pylori* infection (**Figures 7G,H**) despite its inability to induce hypersegmentation (**Figures 4A,B**), and these two treatments had no additional effect on nuclear volume when used in

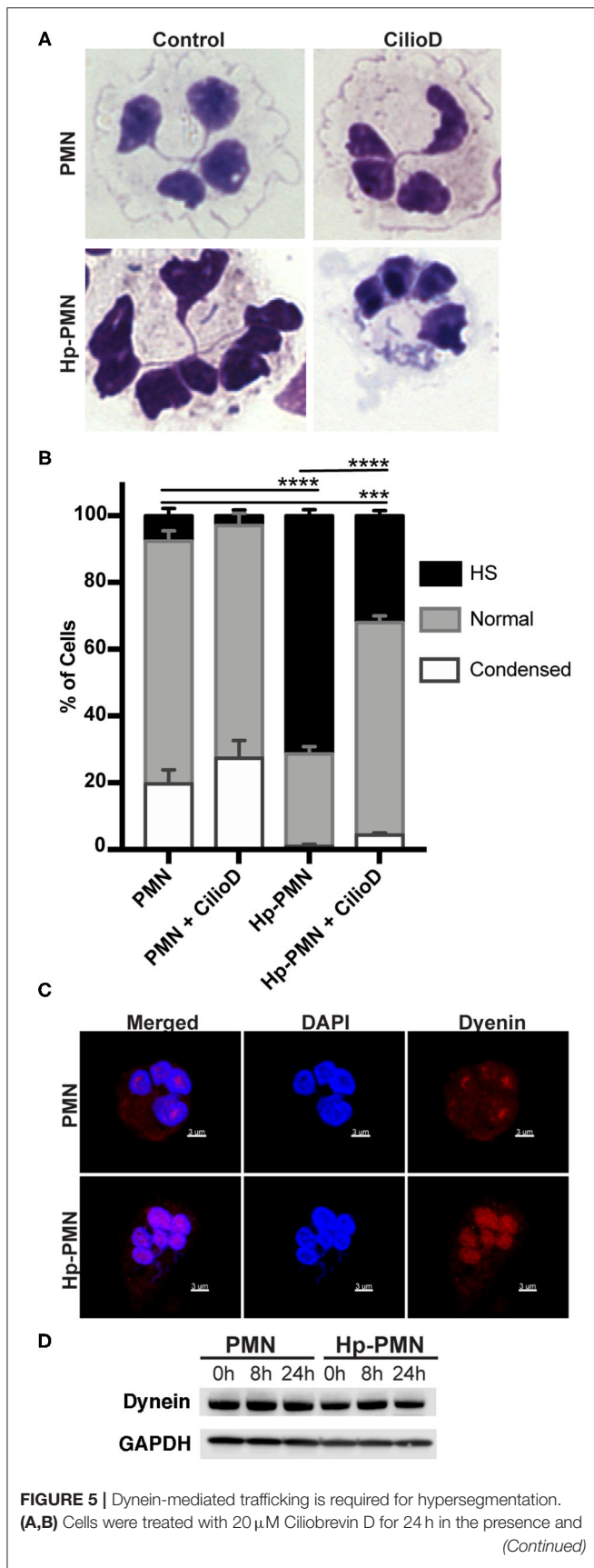


**FIGURE 5 |** absence of *H. pylori*. Nuclear morphology was scored by light microscopy after Hema-3 staining. Representative images (A) and pooled data (B) are shown. Graphs indicate the mean + standard error of the mean. Significant differences in hypersegmentation (HS) were determined using two-way ANOVA and Tukey's multiple comparison test.  $***P \leq 0.001$ ,  $****P \leq 0.0001$ ,  $n = 3$ . (C) Dynein localization shown in reconstructed confocal Z-stacks of cells stained with DAPI (blue) and anti-dynein antibodies (Alexa Fluor 549 secondary antibody, red). Scale bar = 3  $\mu$ m ( $\times 1,000$  original magnification). (D) Dynein immunoblot of infected and uninfected cell lysates at 0, 8, and 24 h timepoints and the loading control GAPDH.

combination. Altogether, our data demonstrate that PMN nuclei enlarged significantly prior to hypersegmentation, that these two processes can be uncoupled, and that they depended on MTs to different extents.

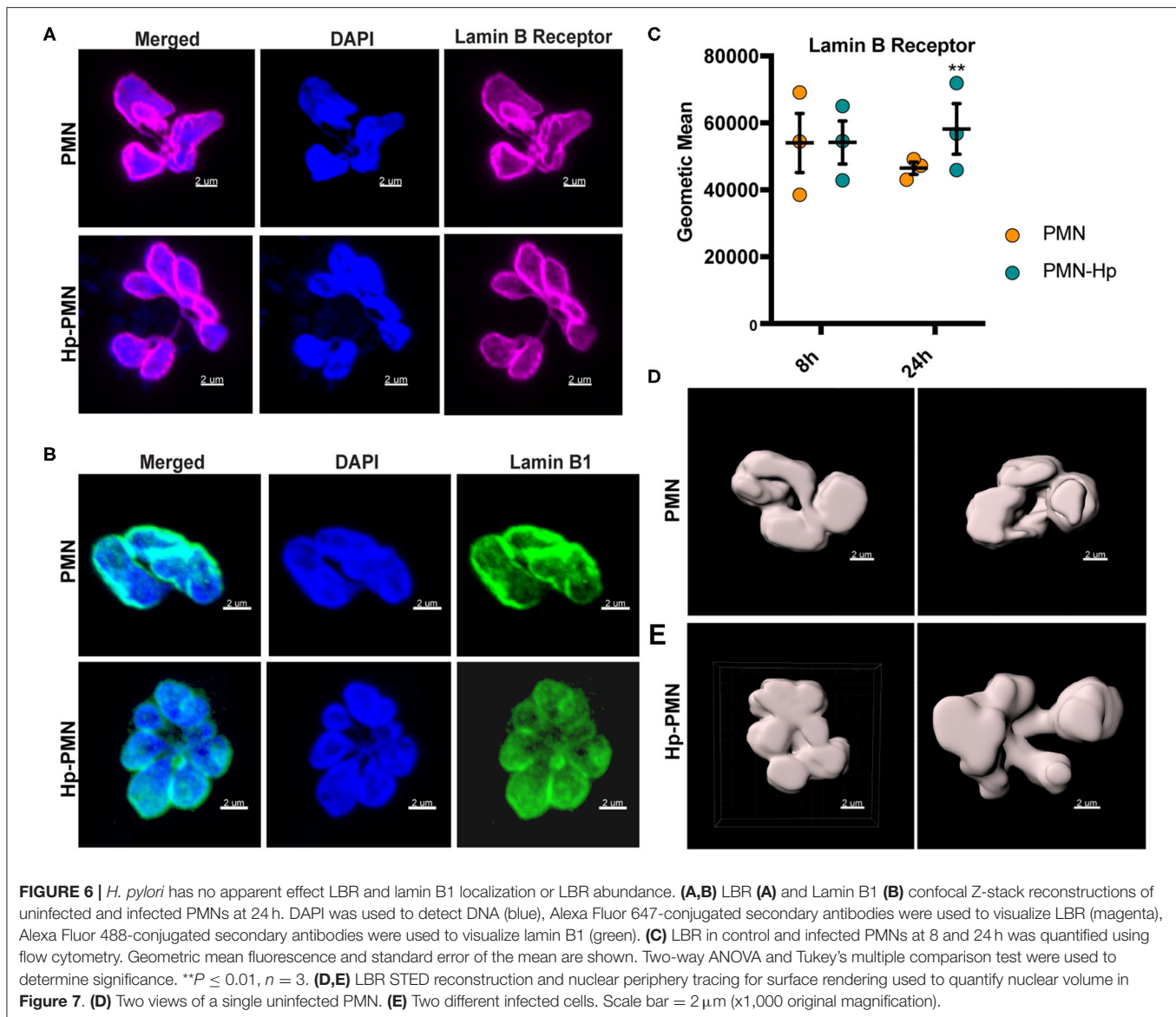
### DISCUSSION

Relatively little is known about the mechanisms that control neutrophil nuclear morphology. Until recently, PMN hypersegmentation was believed to be a rare event that arose primarily in the context of folate or vitamin B12 deficiency or as a consequence of mutations leading to triplication of *LBR* (18, 34). However, since the discovery of PMN plasticity it has become apparent that hypersegmentation is a defining feature of neutrophils in many microenvironments and disease states, including several types of cancer and acute as well as chronic inflammation (5, 9–12, 15, 16). Nonetheless, how hypersegmentation is achieved and the functional consequences of this unusual nuclear morphology are unknown. The results of this study provide significant insight into the molecular mechanisms that mediate hypersegmentation of mature human neutrophils during *H. pylori* infection. Our data reveal a prominent role for MT dynamics and dynein activity in this process and clearly show that hypersegmentation can be achieved without changes in DNA content or *LBR* abundance.

In most non-dividing cells MTs are relatively stable with half-lives of 5–20 min (35). In marked contrast, neutrophil MTs are highly dynamic, exhibit extensive tyrosination, and have a calculated half-life of only 15–30 s (35). Herein, we demonstrated that dynamic, tyrosinated MTs increased markedly in number and length after *H. pylori* infection. Sensitivity to inhibition by nocodazole and taxol at early and late time points demonstrated that MT dynamics were required to induce and maintain hypersegmentation, and accelerated MT rearrangement following taxol removal suggests that MT dynamics were enhanced. Z-stack images and videos show that MTs emanating from the MTOC extended between and around nuclear lobes of both control and infected neutrophils. Nevertheless, we also show that MTs are not required to sustain the normal, lobed morphology of mature PMNs, in agreement with published data (35). These data reinforce the fact that mechanisms of segmentation and hypersegmentation are distinct.

The ability of MTs to exert force on the nucleus is established and the results of this study support a model of





hypersegmentation driven by mechanotransduction across the nuclear envelope. MTs interact with nuclei by one of two mechanisms. Typically, MTs bind directly to LINC (Linker of Nucleoskeleton and Cytoskeleton) complex proteins in the nuclear membrane which are, in turn, connected to lamin A, its splice variant lamin C and chromatin. As nuclei of most cells are relatively rigid, force exerted by MTs is utilized for nuclear rotation and positioning (18, 36). During neutrophil development lamin A/C and essential components of the LINC complex are downregulated and disappear, and therefore cannot account for hypersegmentation in our system despite the central role of lamin A/C downregulation in nuclear deformability (18).

Dynein is a motor protein and AAA<sup>+</sup> ATPase that mediates retrograde transport and also allows MTs to exert force on other cellular structures. At the onset of mitosis, dynein is recruited to the surface of prophase nuclei and in this locale regulates

focal polymerization of MTs that invaginate the nuclear envelope adjacent to the MTOC and exert a pulling force that culminates in catastrophic membrane rupture (37). Although the essential role of dynein in mitosis is unequivocal, its ability to interact with interphase nuclei has only recently been described (38, 39). It has been proposed that dynein may interact preferentially with tyrosinated MTs, and in melanoma cell lines nocodazole enhances dynein nuclear accumulation (38, 39). In contrast, we show here that dynein is distributed diffusely throughout human PMNs, confirming results of Huang et al. (33), yet accumulated at the nucleus after *H. pylori* infection. As dynein activity and MT dynamics were required for hypersegmentation, we propose that processes typically utilized for nuclear envelope breakdown in mitosis may be repurposed to induce hypersegmentation during *H. pylori* infection. Notably, dynein connects MTs to nuclei not *via* LINC complexes but rather *via* interactions with nuclear pore

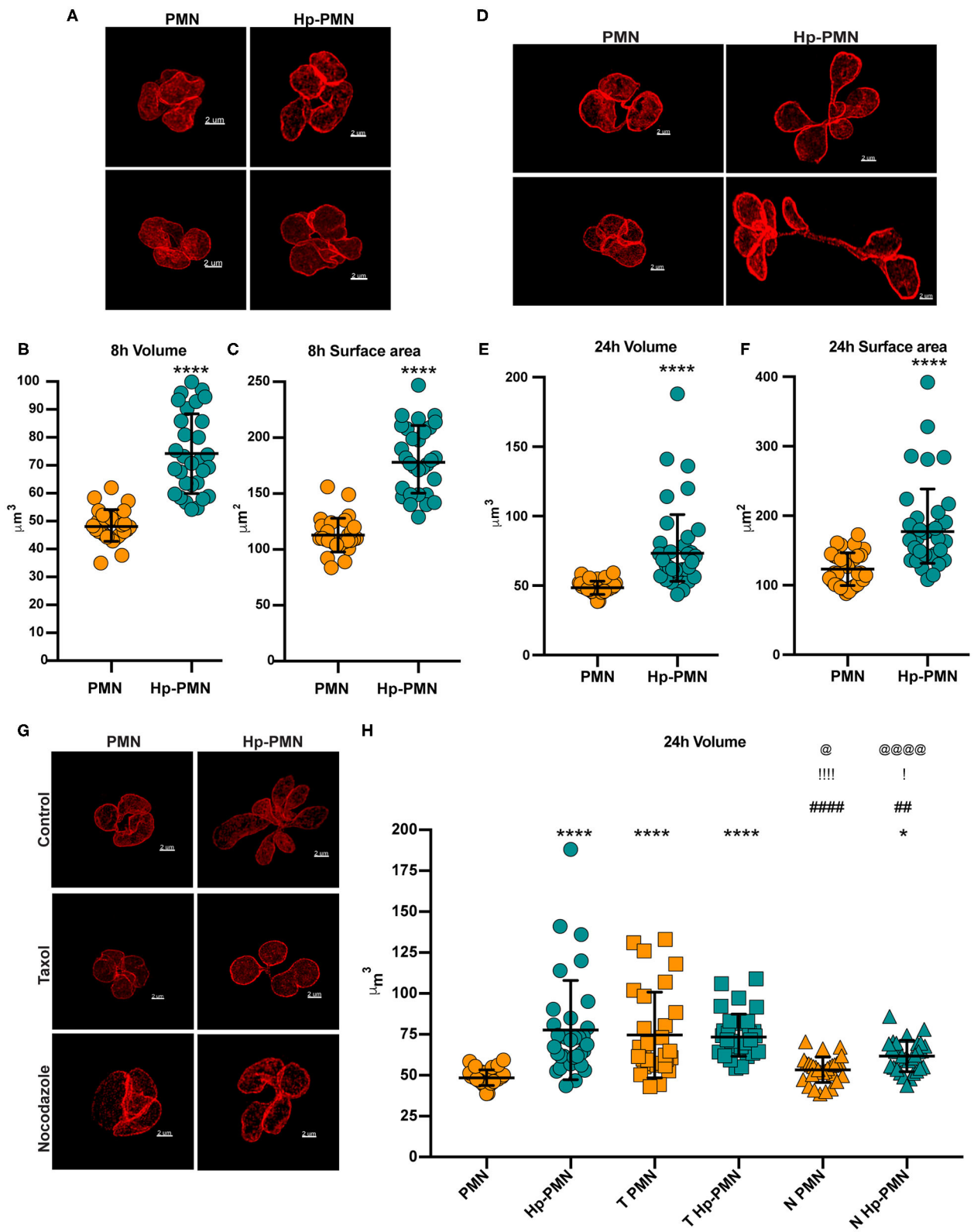


**FIGURE 7 |** *H. pylori* infection and microtubule dynamics alter nuclear volume. Uninfected and infected PMNs were stained to detect LBR (red) after 8 h (A–C) or 24 h (D–H). As indicated in (G,H), cells were also treated with taxol (T) or nocodazole (N) at time zero. (A,D,G) Representative 3D reconstructions of STED Z-stacks. Scale (Continued)

**FIGURE 7** | bar = 2 $\mu$ m (x1,000 original magnification). Quantification of nuclear volume (**B,E,H**) and surface area (**C,F**) were done by tracing the nuclear periphery on each stack using the volume Imaris extension as shown in **Figure 6D** (see also **Supplementary Videos 5, 6**). Ten cells were analyzed per donor, per condition.  $n = 3$ . Graphs show the mean  $\pm$  SD along with data for individual cells. Statistical significance was determined by two-way ANOVA and Tukey's multiple comparison test. \*\*\*\* $P \leq 0.0001$  and \* $P \leq 0.05$  vs. PMN. #### $P \leq 0.0001$  and ## $P \leq 0.01$  vs. Hp-PMN. !!! $P \leq 0.0001$  and ! $P \leq 0.05$  vs. T- PMN. @@@@ $P < 0.0001$ , @ $P \leq 0.05$  vs. T Hp-PMN.

complexes and Ran binding protein 2 (40). Mechanisms that govern the magnitude and duration of dynein accumulation on interphase nuclei remain to be determined.

In the context of this study, we used STED super-resolution microscopy and LBR staining to analyze neutrophil nuclear morphology in unprecedented detail and our data demonstrate that nuclei enlarged significantly prior hypersegmentation. Model systems commonly used for studies of nuclear size regulation include cancer cells, *Xenopus* oocytes, yeast, plants, neurons, fibroblasts and several cell lines (41–44). Although the mechanisms are only partially understood, it is clear that chromatin organization and the magnitude of nuclear import are critical players (41, 42). Conversely, DNA abundance is largely non-contributory, and roles for MTs are context and cell type-specific (41–43). For example, MTs constrain nuclear size in mesenchymal stem cells, have no effect on L929 cells, and collaborate with dynein for nuclear expansion in *Xenopus* oocytes (43, 44). At a minimum, MTs can influence nuclear size by delivering cargo to the import machinery in the vicinity of nuclear pores and by exerting force on the nuclear envelope that can, in and of itself, alter chromatin structure and change gene expression (39, 40, 45). Although similar studies of neutrophils have not been performed, it is of interest that heterochromatin, which is abundant in PMNs, is tethered to the lamina by LBR whereas euchromatin interacts with nuclear pore complexes (18). Whether chromatin organization or nuclear transport pathways are modulated in our system remains to be determined, but data presented here show that bacteria-triggered nuclear enlargement was inhibited by nocodazole and can be recapitulated by taxol in the absence of infection; and our published data show that gene expression and protein synthesis are required for hypersegmentation (16). Thus, it is attractive to predict that transcriptional reprogramming as well as nuclear size and morphology may be inherently linked at the level of MT-driven mechanotransduction. Elucidating the effects of *H. pylori* on neutrophil gene expression, chromatin structure and nuclear transport are areas of active investigation in our laboratory.

The significance of hypersegmentation with respect to neutrophil function and fate, and whether other bacterial pathogens induce a similar phenotype are unknown. It is often stated that a segmented nucleus may facilitate neutrophil migration through tight spaces (18, 46, 47). Accordingly, we are using a multifaceted approach to elucidate effects on hypersegmentation on neutrophil migration, and preliminary results suggest that this process is impaired rather than enhanced (Prichard et al., unpublished data). Thus, it is conceivable that hypersegmentation together with extended lifespan may contribute to PMN accumulation in the gastric mucosa during *H. pylori* infection. We are also actively pursuing

the possibility that nuclear enlargement and hypersegmentation may be hallmarks of chromatin reorganization and changes in gene expression occurring on a scale greater than is typically observed in neutrophils and which may, in turn, influence PMN immunoregulatory properties as well as the mode and efficiency of PMN death. To our knowledge, hypersegmentation has not yet been reported in the context of other infections, and it will be important to determine if this phenotype is specific for *H. pylori*. To this end, we have shown that *Francisella tularensis* does not alter neutrophil nuclear morphology despite its ability to replicate in the cytosol and prolong cell lifespan (23), and pilot studies by our group suggest that hypersegmentation does not occur in the context of neutrophil infection with *Neisseria gonorrhoeae* or *Staphylococcus aureus*. Additional studies of viral, bacterial, fungal, and parasitic pathogens are clearly needed, and it is tempting to speculate that nuclear morphology may receive more attention in the future as one aspect of the rapidly expanding neutrophil plasticity field.

In summary, we identified a new mechanism of neutrophil hypersegmentation that is driven by MT dynamics and dynein. To achieve this, we capitalized on the tractability of our *in vitro* *H. pylori* infection model and it will of interest in future studies to determine if this mechanism is conserved in other hypersegmented neutrophil populations and subsets. Based on our results, we propose that dynein is responsible for connecting MTs to the nucleus and that MTs interacting with dynein force the enlarged nucleus to hypersegment *via* mechanotransduction across the membrane and by repurposing molecular mechanisms that elicit nuclear rupture at the onset of mitosis in other cell types. Whether these processes are coupled to chromatin rearrangements or are essential for neutrophil transcriptional reprogramming during *H. pylori* infection remain to be determined. In future studies it will also be important to determine if the nuclear morphology of individual cells is static or dynamic, to identify sources of membrane used for nuclear expansion, and to investigate signals that modulate MT abundance.

## DATA AVAILABILITY STATEMENT

The raw data supporting the conclusions of this article will be made available by the authors, without undue reservation.

## ETHICS STATEMENT

The studies involving human participants were reviewed and approved by Institutional Review Board of the University of

Iowa. The patients/participants provided their written informed consent to participate in this study.

## AUTHOR CONTRIBUTIONS

L-AHA conceived of the study, designed experiments, analyzed data and co-wrote the manuscript. SLS-DT designed and performed experiments, analyzed data and co-wrote the manuscript. All authors contributed to the article and approved the submitted version.

## FUNDING

This work was supported by funds from the National Institutes of Health, NIAID R01 AI119965 and VA Merit Review Grant 1I01BX002108 awarded to L-AHA as well as a National Science Foundation predoctoral fellowship #1546595 awarded to SLS-DT.

## REFERENCES

- Nauseef WM, Borregaard N. Neutrophils at work. *Nat Immunol.* (2014) 15:602–11. doi: 10.1038/ni.2921
- Nauseef WM. Neutrophils, from cradle to grave and beyond. *Immunol Rev.* (2016) 273:5–10. doi: 10.1111/imr.12463
- Kruger P, Saffarzadeh M, Weber AN, Rieber N, Radsak M, von Bernuth H, et al. Neutrophils: Between host defence, immune modulation, tissue injury. *PLoS Pathog.* (2015) 11:e1004651. doi: 10.1371/journal.ppat.1004651
- Beyrau M, Bodkin JV, Nourshargh S. Neutrophil heterogeneity in health and disease: a revitalized avenue in inflammation and immunity. *Open Biol.* (2012) 2:120134. doi: 10.1098/rsob.120134
- Fridlender ZG, Sun J, Kim S, Kapoor V, Cheng G, Ling L, et al. Polarization of tumor-associated neutrophil phenotype by TGF-beta: "N1" versus "N2" TAN. *Cancer Cell.* (2009) 16:183–94. doi: 10.1016/j.ccr.2009.06.017
- Silvestre-Roig C, Fridlender ZG, Glogauer M, Scapini P. Neutrophil diversity in health and disease. *Trends Immunol.* (2019) 40:565–83. doi: 10.1016/j.it.2019.04.012
- Giese MA, Hind LE, Huttenlocher A. Neutrophil plasticity in the tumor microenvironment. *Blood.* (2019) 133:2159–67. doi: 10.1182/blood-2018-11-844548
- Jaillon S, Ponzetta A, Di Mitri D, Santoni A, Bonocchi R, Mantovani A. Neutrophil diversity and plasticity in tumour progression and therapy. *Nat Rev Cancer.* (2020) 20:485–503. doi: 10.1038/s41568-020-0281-y
- Eruslanov EB, Bhojnarwal PS, Quatromoni JG, Stephen TL, Ranganathan A, Deshpande C, et al. Tumor-associated neutrophils stimulate T cell responses in early-stage human lung cancer. *J Clin Invest.* (2014) 124:5466–80. doi: 10.1172/JCI77053
- Singel KL, Emmons TR, Khan ANH, Mayor PC, Shen S, Wong JT, et al. Mature neutrophils suppress T cell immunity in ovarian cancer microenvironment. *JCI Insight.* (2019) 4:311. doi: 10.1172/jci.insight.122311
- Lokwani R, Wark PAB, Baines KJ, Barker D, Simpson JL. Hypersegmented airway neutrophils and its association with reduced lung function in adults with obstructive airway disease: an exploratory study. *BMJ Open.* (2019) 9:e024330. doi: 10.1136/bmjopen-2018-024330
- Brown RA, Henderlight M, Do T, Yasin S, Grom AA, DeLay M, et al. Neutrophils from children with systemic juvenile idiopathic arthritis exhibit persistent proinflammatory activation despite long-standing clinically inactive disease. *Front Immunol.* (2018) 9:2995. doi: 10.3389/fimmu.2018.02995

## ACKNOWLEDGMENTS

The authors acknowledge use of the University of Iowa Central Microscopy Research Facility, a core resource supported by the University of Iowa Office of the Vice President for Research and the Carver College of Medicine. Acquisition of the Leica SP8 laser-scanning confocal microscope with STED capability was made possible by a generous grant from the Roy J. Carver Charitable Trust with additional funding provided by the University of Iowa Office of the Vice President for Research, the Carver College of Medicine and the College of Liberal Arts and Sciences. Technical assistance was provided by Mr. Tom Moninger and Dr. Chantal Allamargot.

## SUPPLEMENTARY MATERIAL

The Supplementary Material for this article can be found online at: <https://www.frontiersin.org/articles/10.3389/fimmu.2021.653100/full#supplementary-material>

- Im DD, Ho CH, Chan RY. Hypersegmented neutrophils in an adolescent male with heatstroke. *J Pediatr Hematol Oncol.* (2015) 37:488. doi: 10.1097/MPH.0000000000000356
- Friedman EW, Williams JC, Predergast E. Polymorphonuclear leucocyte hypersegmentation in heat stroke. *Br J Haematol.* (1982) 50:168–76. doi: 10.1111/j.1365-2141.1982.tb01901.x
- Pillay J, Kamp VM, van Hoffen E, Visser T, Tak T, Lammers JW, et al. A subset of neutrophils in human systemic inflammation inhibits T cell responses through Mac-1. *J Clin Invest.* (2012) 122:327–36. doi: 10.1172/JCI57990
- Whitmore LC, Weems MN, Allen LAH. Cutting Edge: Helicobacter pylori induces nuclear hypersegmentation subtype differentiation of human neutrophils *in vitro*. *J Immunol.* (2017) 198:1793–7. doi: 10.4049/jimmunol.1601292
- Ohms M, Moller S, Laskay T. An attempt to polarize human neutrophils toward N1 and N2 phenotypes *in vitro*. *Front Immunol.* (2020) 11:532. doi: 10.3389/fimmu.2020.00532
- Manley HR, Keightley MC, Lieschke GJ. The neutrophil nucleus: an important influence on neutrophil migration and function. *Front Immunol.* (2018) 9:2867. doi: 10.3389/fimmu.2018.02867
- Bills T, Spatz L. Neutrophilic hypersegmentation as an indicator of incipient folic acid deficiency. *Am J Clin Pathol.* (1977) 68:179–84. doi: 10.1093/ajcp/68.2.263
- Thompson WG, Cassino C, Babitz L, Meola T, MBERMAN R, Lipkin MJ, et al. Hypersegmented neutrophils and vitamin B12 deficiency. *Acta Haematol.* (1989) 81:186–91. doi: 10.1159/000205559
- Allen LAH, Schlesinger LS, Kang B. Virulent strains of Helicobacter pylori demonstrate delayed phagocytosis and stimulate homotypic phagosome fusion in macrophages. *J Exp Med.* (2000) 191:115–27. doi: 10.1084/jem.191.1.115
- Nauseef WM. Isolation of human neutrophils from venous blood. *Methods Mol Biol.* (2007) 412:15–20. doi: 10.1007/978-1-59745-467-4\_2
- Schwartz JT, Barker JH, Kaufman J, Fayram DC, McCracken JM, Allen LAH. Francisella tularensis inhibits the intrinsic extrinsic pathways to delay constitutive apoptosis prolong human neutrophil lifespan. *J Immunol.* (2012) 188:3351–63. doi: 10.4049/jimmunol.1102863
- Allen LAH, Beecher BR, Lynch JT, Rohner OV, Wittine LM. Helicobacter pylori disrupts NADPH oxidase targeting in human neutrophils to induce extracellular superoxide release. *J Immunol.* (2005) 174:3658–67. doi: 10.4049/jimmunol.174.6.3658
- Allen LAH. Immunofluorescence and confocal microscopy of neutrophils. *Methods Mol Biol.* (2014) 1124:251–68. doi: 10.1007/978-1-62703-845-4\_16

26. Ding M, Robinson JM, Behrens BC, Vandre DD. The microtubule cytoskeleton in human phagocytic leukocytes is a highly dynamic structure. *Eur J Cell Biol.* (1995) 66:234–45.
27. McCracken JM, Kinkead LC, McCaffrey RL, Allen LAH. Francisella tularensis modulates a distinct set of regulatory factors sustains mitochondrial integrity to impair human neutrophil apoptosis. *J Innate Immun.* (2016) 8:299–313. doi: 10.1159/000443882
28. Magiera MM, Janke C. Post-translational modifications of tubulin. *Curr Biol.* (2014) 24:R351–R4. doi: 10.1016/j.cub.2014.03.032
29. Wiese C, Zheng Y. Microtubule nucleation: gamma-tubulin and beyond. *J Cell Sci.* (2006) 119:4143–53. doi: 10.1242/jcs.03226
30. Schliwa M, Pryzwansky KB, Euteneuer U. Centrosome splitting in neutrophils: an unusual phenomenon related to cell activation and motility. *Cell.* (1982) 31:705–17. doi: 10.1016/0092-8674(82)90325-7
31. Tanenbaum ME, Akhmanova A, Medema RH. Bi-directional transport of the nucleus by dynein and kinesin. *Commun Integr Biol.* (2011) 4:21–5. doi: 10.4161/cib.13780
32. Firestone AJ, Weinger JS, Maldonado M, Barlan K, Langston LD, O'Donnell M, et al. Small-molecule inhibitors of the AAA+ ATPase motor cytoplasmic dynein. *Nature.* (2012) 484:125–9. doi: 10.1038/nature10936
33. Huang, J.-B., Espinoza J, Romero R, Petty HR. Apparent role of dynein in glucose-6-phosphate dehydrogenase trafficking in neutrophils from pregnant women. *Metabolism.* (2006) 55:279–81. doi: 10.1016/j.metabol.2005.09.002
34. Gravemann S, Schnipper N, Meyer H, Vaya A, Nowaczyk MJM, Rajab A, et al. Dosage effect of zero to three functional LBR-genes *in vivo* and *in vitro*. *Nucleus.* (2010) 1:179–89. doi: 10.4161/nucl.1.2.11113
35. Ding M, Robinson JM, Behrens BC, Vandre DD. The microtubule cytoskeleton in human phagocytic leukocytes is a highly dynamic structure. *Eur J Cell Biol.* (1995) 66:234–45.
36. Keeling MC, Flores LR, Dodhy AH, Murray ER, Gavara N. Actomyosin and vimentin cytoskeletal networks regulate nuclear shape, mechanics and chromatin organization. *Sci Rep.* (2017) 7:5219. doi: 10.1038/s41598-017-05467-x
37. Salina D, Bodoor K, Eckley DM, Schroer TA, Rattner JB. Cytoplasmic dynein as a facilitator of nuclear envelope breakdown. *Cell.* (2002) 98:97–107. doi: 10.1016/S0092-8674(01)00628-6
38. Jodoin JN, Shboul M, Sitaram P, Zein-Sabatto H, Reversade B, Lee E, et al. Human Asunder promotes dynein recruitment and centrosomal tethering to the nucleus at mitotic entry. *Mol Biol Cell.* (2012) 23:4713–24. doi: 10.1091/mbc.e12-07-0558
39. Gerlitz G, Reiner O, Bustin M. Microtubule dynamics alter the interphase nucleus. *Cell Mol Life Sci.* (2013) 70:1255–68. doi: 10.1007/s00018-012-1200-5
40. Maizels Y, Gerlitz G. Shaping of interphase chromosomes by the microtubule network. *FEBS J.* (2015) 282:3500–24. doi: 10.1111/febs.13334
41. Edens LJ, White KH, Jevtic P, Li X, Levy DL. Nuclear size regulation: from single cells to development and disease. *Trends Cell Biol.* (2013) 23:151–9. doi: 10.1016/j.tcb.2012.11.004
42. Jevtic P, Levy DL. Mechanisms of nuclear size regulation in model systems and cancer. *Adv Exp Med Biol.* (2014) 773:537–69. doi: 10.1007/978-1-4899-8032-8\_25
43. Doolin MT, Ornstein TS, Stroka KM. Nuclear deformation in response to mechanical confinement is cell type dependent. *Cells.* (2019) 8:427. doi: 10.3390/cells8050427
44. Mukherjee RN, Chen P, Levy DL. Recent advances in understanding nuclear size and shape. *Nucleus.* (2016) 7:167–86. doi: 10.1080/19491034.2016.1162933
45. Shekhar N, Wu J, Dickinson RB, Lele TP. Cytoplasmic dynein: tension generation on microtubules and the nucleus. *Cell Mol Bioeng.* (2013) 6:74–81. doi: 10.1007/s12195-012-0257-4
46. Hoffmann K, Sperling K, Olins AL, Olins DE. The granulocyte nucleus and lamin B receptor: avoiding the ovoid. *Chromosoma.* (2007) 116:227–35. doi: 10.1007/s00412-007-0094-8
47. Salvermoser M, Begandt D, Alon R, Walzog B. Nuclear deformation during neutrophil migration at sites of inflammation. *Front Immunol.* (2018) 9:2680. doi: 10.3389/fimmu.2018.02680

**Conflict of Interest:** The authors declare that the research was conducted in the absence of any commercial or financial relationships that could be construed as a potential conflict of interest.

Copyright © 2021 Silva-Del Toro and Allen. This is an open-access article distributed under the terms of the Creative Commons Attribution License (CC BY). The use, distribution or reproduction in other forums is permitted, provided the original author(s) and the copyright owner(s) are credited and that the original publication in this journal is cited, in accordance with accepted academic practice. No use, distribution or reproduction is permitted which does not comply with these terms.